Research Article

Journal of Environmental Nanotechnology

Characterization and Ambient Temperature Hydrogen Sulfide Sensing of Annealed NiO-MnO_2 Thin Films Prepared via Jet Nebulizer Spray Pyrolysis

S. Saranya[1], N. Sethupathi[2*], P. Mahalingam[2] and P. Sivakumar[2]

[1]Department of Physics, Arignar Anna Government Arts College, Namakkal, TN, India

[2]Department of Chemistry, Arignar Anna Government Arts College, Namakkal, TN, India

Received: 28.06.2024 Accepted: 23.08.2024 Published: 30.09.2024

*sethupathi2011@gmail.com

ABSTRACT

A jet nebulizer spray pyrolysis technique to synthesize NiO-MnO_2 thin films was demonstrated. These nanosheets were annealed at 350, 450 and 550 °C for 2 hours. The thin films surface morphology and structure were characterized using scanning electron microscopy, XRD, and UV spectroscopy. Subsequently, utilized as gas sensors for the detection of hydrogen sulphide gas. The introduction of NiO into MnO_2 nanosheets significantly improved the gas-sensing performance. Notably, the gas-sensing response of the NiO-MnO_2 nanosheet sensor surpassed that of both NiO and MnO_2 alone, reaching a notable value of 165 when detecting 100 ppm hydrogen sulfide gas with the NiO-MnO_2 thin film sensor. A remarkable feature of the NiO-MnO_2 thin film sensor is its accelerated response time, registering at 10 seconds when exposed to 100 ppm of hydrogen sulfide gas. The mechanism underlying gas sensing and the factors contributing to the enhanced gas response of NiO-MnO_2 thin film is thoroughly discussed. From a broader perspective, these developed sensors present a novel platform for the identification and monitoring of hydrogen sulfide gas, showcasing significant advancements in gas-sensing technology.

Keywords: Metal oxide; Thin films; Sensor; H_2S.

1. INTRODUCTION

Thin films are essential components in diverse technological applications owing to their distinctive properties and versatile functionalities. These films consist of thin layers of material deposited on substrates, typically ranging from a few nanometers to several micrometers in thickness. Their significance in fields such as energy storage, catalysis, and optoelectronics is derived from their ability to display tailored properties that differ from those of bulk materials (Guisbiers *et al*. 2012). This characteristic allows for precise engineering of film properties to meet specific applications.

In recent years, composite nanomaterials, which demonstrate enhanced sensing performance compared to individual components, have garnered significant interest in the field of gas sensors. This interest is driven by the synergistic effects resulting from the coupling of two distinct classes of nanomaterials (Walker *et al*. 2019). The properties of these nanomaterial composites are not merely a sum of the characteristics of their individual components; instead, they exhibit complex and superior behaviors. Several researches highlight the potential of composite nanostructured thin films in advancing gas sensing technologies (Betty *et al*. 2023). Among these composite materials, NiO-SnO_2 nanostructures have been extensively investigated for their gas sensing characteristics (Hu *et al*. 2018). Nickel oxide (NiO) is a p-type semiconductor with an energy gap of 4.2 eV. Research efforts have focused on studying the gas sensing performance of various NiO-SnO_2 nanostructures, demonstrating enhanced sensitivities compared to sensors based on single-component materials (Din *et al*. 2020). The NiO thin films deposited by d.c. reactive magnetron sputtering demonstrated strong sensitivity to NO_2 concentrations ranging from 1 to 10 ppm, highlighting their potential for effective gas sensing applications at moderate temperatures. SiO_2 sol–gel mesoporous thin films incorporating NiO nanoparticles demonstrate their versatility and suitability for environmental monitoring and industrial safety purposes (Della *et al*. 2011).

A range of sensors utilizing manganese dioxide (MnO_2) nanostructures have been explored for the detection of diverse molecules. The structural flexibility and varied oxidation states of manganese present in MnO_2 nanostructures play a crucial role in enhancing their effectiveness in sensing applications. Manganese oxide-based nanomaterials like nickel manganite ($NiMn_2O_4$) (He *et al*. 2011), Mn-Co-Ni-O nanofilms (Huang *et al*. 2015), Mn_3O_4 nanomaterials have been prepared by researchers through different procedures and

characterized for its sensing application for various molecules. These MnO_2-based sensors demonstrate promising potential for detecting molecules such as acetaldehyde (Balamurugan *et al*. 2015), ammonia (Kumar *et al*. 2016), H_2S (Chaudhari *et al*. 2006) with high sensitivity and specificity, offering valuable contributions to the field of medical diagnostics and environmental monitoring. The structural versatility of MnO_2 nanostructures opens avenues for further advancements in sensor design and development.

In addition to morphological tailoring, enhancing the functionality of bare Mn–Oxide gas sensors through sensitization with appropriate metal/oxide agents represents an effective approach. This strategy aims to leverage synergistic chemical and electronic effects to achieve improved sensor performance at moderate operating temperatures. The current study explores the structural, morphological, optical, and electrical properties of annealed NiO-MnO_2 thin films prepared using jet nebulizer spray pyrolysis technique, as well as investigates the hydrogen sulfide sensing characteristics of the thin film at ambient temperature.

2. EXPERIMENTAL APPROACH

Thin films of nickel oxide-manganese oxide were prepared on a glass substrate using jet nebulizer spray pyrolysis technique (Sethupathi *et al*. 2012). The glass plates underwent thorough cleaning with double-distilled water to eliminate any remaining impurities. Subsequently, the plates were immersed in a 2N nitric acid solution to remove oxide impurities on the glass substrate surface. After each acid treatment, the substrate was washed with double-distilled water and dried well, and this purification process was repeated three times to ensure complete removal of impurities.

For the film deposition, 0.2 M stock solutions of nickel acetate ($Ni(CH_3COO)_2$) and manganese acetate tetrahydrate ($(CH_3COO)_2Mn.4H_2O$) were prepared using analytic grade chemicals. Mixing appropriate quantities of nickel acetate and manganese acetate tetrahydrate solutions, 4 % of nickel containing thin film deposit was achieved. The resulting mixture was stirred and ultrasonicated for 10 minutes to homogenize the solution. Subsequently, 8 ml of the composition mixture was introduced into a nebulizer, with the top attached to a custom glass container tube. The nebulizer's bottom was connected to a compressed air flow set at 4 atmosphere pressures. The compressed air converted the solution into mists, which were directed through a guiding glass tube onto the preheated (300 °C) and well-cleaned glass substrate. At this temperature, the mist underwent pyrolytic decomposition, forming metal oxide thin films. The resulting thin films were annealed at temperatures of 350, 450, and 550 °C for 2 hours. The influence of various annealing temperatures on nickel oxide - manganese oxide thin films morphology, structural and sensing properties were examined using XRD, UV-VIS, SEM, and a sensor system.

A NiO-MnO_2 thin film was deposited onto glass substrates. Silver (Ag) paste was employed to establish ohmic contacts. This study utilized hydrogen sulfide gas as the target analyte. Resistance changes upon exposure to the gas were monitored using a Keithley digital multimeter (DMM7510). The sensitivity of the gas is defined as

$$S_r = \frac{(R_g - R_a)}{R_a} X\ 100\ \% \quad (1)$$

where, R_g is the resistance in the presence of a target gas and R_a is the resistance in air (Zao *et al*., 2008). The response time is defined as the time required to reach 90% of the response signal, while the recovery time(s) denotes the time needed to recover 90 % of the original baseline signal. The gas sensor was allowed to stabilize at the operating temperature 250 °C in air for 2 hours. The prepared thin film was exposed with hydrogen sulfide gas concentration of 100 ppm at optimum operating temperature of 250 °C. Dry air was introduced to cleanse the gas chamber of residual gas content. Practical gas testing involved adjusting the target gas concentration by diluting it with synthetic air. Dry synthetic air was employed to achieve desired gas concentrations and to purge the gas chamber before and after exposure to the test gas. Resistance measurements were conducted for NiO-MnO_2 thin films annealed at 350. 450 and 550 °C. The sensor is integrated into a four-probe setup for precise resistance measurements. The sensing characteristics are determined by analyzing the observed changes in resistance.

3. RESULTS AND DISCUSSION

3.1 FESEM

Figure 1 shows the FESEM image of NiO-MnO_2 thin layer composite annealed at 350, 450 and 550 °C. The thin film prepared by annealing at 350 and 450 °C shows the amorphous nature. The thin layer annealed at 550 °C exhibits well connected particles with porous structure. The average length and width of the agglomerated particles of the thin layer annealed at 550 °C are 300 nm and 130 nm. The crystallinity of the thin layer increased with increasing annealing temperature. This porous thin film morphology is suitable for gas sensing because the analytes can penetrate the thin film surface, and interact with reactive sites spread over larger surface area.

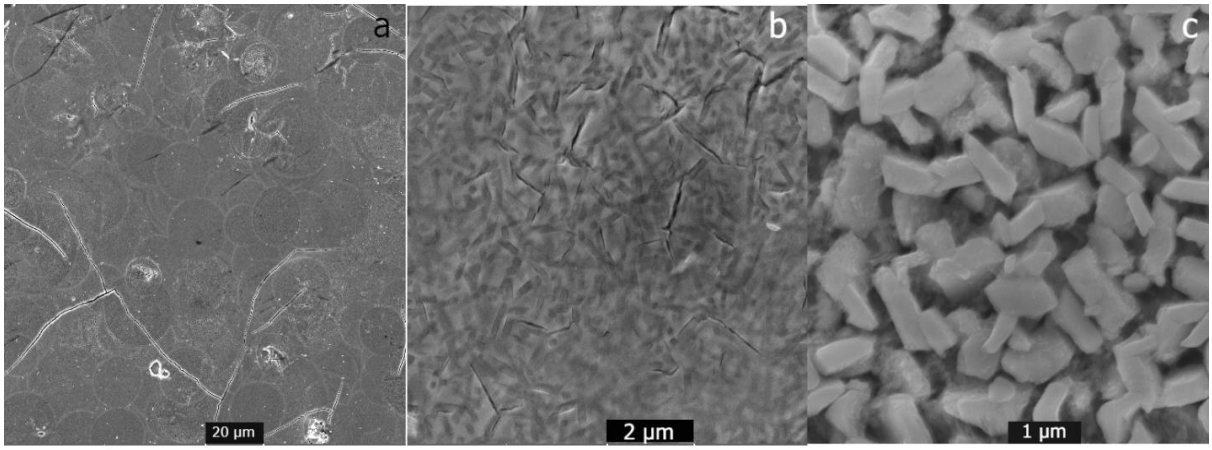

Fig. 1: FESEM image of NiO-MnO_2 thin layer composite annealed at a) 350, b) 450 and c) 550 °C

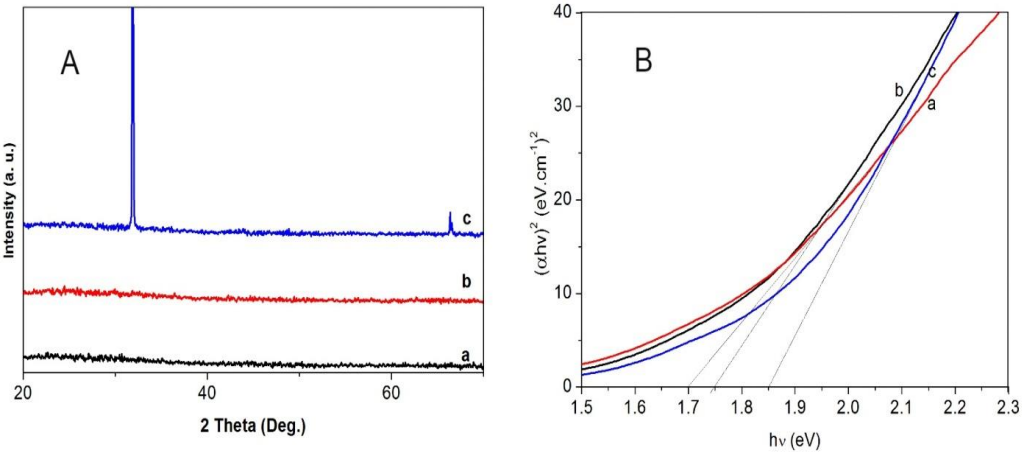

Fig. 2: A) XRD Pattern and B) Tauc'S Plot of NiO-MnO2 thin films annealed at 350 (a), 450 (b) and 550 (c) °C

3.2 XRD

Figure 2 (A) illustrates the X-ray diffraction (XRD) pattern of a NiO-MnO_2 thin layer annealed at 350, 450 and 550 °C. The definite sharpening of the XRD peaks in the pattern suggests the crystalline nature of the particles. The diffraction peaks of NiO-MnO_2 annealed at 350 and 450 °C, shown in Figure 2a and Figure 2b, indicate an amorphous nature of the material due to a less-formed crystalline phase. However, at an annealing temperature of 550 °C (Figure 2c), a sharp diffraction peak emerges, suggesting a higher level of crystallization associated with larger crystals (Paine *et al*. 1999). The diffraction peaks observed at 31.89° and 66.35° have been precisely indexed as an orthogonal crystal structure, characterized by lattice constants a = b = 0.324 nm and c = 0.521 nm (JCPDS card no: 00–047-1049). The X-ray diffraction study provides insights into the crystal phase and structural properties of the NiO-MnO_2 material. The XRD pattern of NiO-MnO_2 reveals the presence of the $NiMnO_3$ phase (JCPDS No. 18-0802). To ascertain the particle size of the synthesized NiO-MnO_2 nanoparticles, we employed the Debye-Scherrer formula (Patterson 1939). The calculated average particle size of the sample was found to be 16.21 nm, derived from the FWHM of the more intense peak corresponding to the 101 plane located at 31.89°.

3.3 UV-VIS

The optical absorption spectra of the synthesized NiO-MnO_2 thin film were studied using a UV-Visible spectrophotometer from 200 nm to 800 nm at room temperature. The absorption spectra (not shown) clearly indicate the blue shift for the thin film annealed at higher temperatures. The optical band gap energy of the synthesized thin films were calculated via the Tauc equation, which is given by:

$$\alpha h\nu = A\,(h\nu - E_g)^n \qquad (2)$$

where α is the absorbance coefficient, A is a constant, hν represents the energy of the incident photon, E_g is the band gap energy value of the sample, and the value of n can be 1/2, 2, 3/2, etc., depending on the type of transitions. The value of n is taken to be ½, since this is the case of a direct band gap.

The band gap energy (E_g) has been estimated via plotting the graph of $(\alpha h\nu)^2$ versus hν as shown in Figure 2 (B). The extrapolation of the straight line of $(\alpha h\nu)^2$ to the hν axis gives the band gap energy value (in eV) of the synthesized thin films. The optical band gap of NiO-MnO_2 thin films annealed at 350, 450 and 550 °C are found to be 1.7, 1.75, and 1.85 eV respectively. It can be clearly seen that the optical band gap energy of NiO-MnO_2 thin films increases with the increased annealing temperature. The jet nebulizer spray method emerges as advantageous among the various synthesis techniques for producing NiO-MnO_2 with a band gap of 1.7 – 1.85 eV. This method excels in creating thin films with exceptional uniformity, which is crucial for applications demanding consistent optical and electronic properties across large areas. Its scalability and cost-effectiveness make it well-suited for industrial applications, offering a viable pathway for large-scale production without significant equipment investments (Jagadeesan and Subramaniam 2021). Moreover, the jet nebulizer spray method enables precise control over material composition and structure, ensuring optimal band gap tuning to meet specific technological requirements. This versatility positions it as a preferred choice for sensor applications, highlighting its robust capability to delivering reliable and tailored material properties essential for advancing technology.

3.4 Sensing Performance

The gas sensing performance of thin films is intricately tied to the carrier concentration, a factor closely linked to the annealing temperature of the prepared thin films and the effects of annealing at 350, 450, and 550 °C on NiO-MnO_2 thin films were investigated. Annealing temperature has a significant impact on the sensitivity of thin films, as evidenced by the observed increase in sensitivity with rising temperatures (97 at 350°C, 131 at 450°C, and 165 at 550°C). This effect can be attributed to several factors. Higher annealing temperatures improve the crystal structure and phase formation of the films, leading to better crystallization and more active surface sites, which enhance sensitivity. Additionally, elevated temperatures can increase the grain size of the thin films, potentially improving contact with the analyte and thereby boosting sensitivity; however, excessively large grains may sometimes reduce sensitivity. Furthermore, higher temperatures alter the surface morphology, potentially creating more surface roughness or porous structures, which increase the surface area available for interaction with the analyte. Specifically, the response of these films to 100 ppm H_2S gas at 350 °C was scrutinized. The findings, depicted in Figure 3 (A), distinctly reveal the impact of annealing on these thin films sensing properties. The resistance of the thin film increased significantly upon exposed to H_2S vapor.

The sensitivity of NiO-MnO_2 thin films annealed at 350, 450 and 550 °C were 97, 131, and 165, respectively. The figure clearly demonstrates a gradual increase in response with higher annealing temperatures, suggesting a linear relationship between responses and annealing temperature. When the sensor was exposed to H_2S gas, the sensor resistance increased. In air, the thin film is depleted of electrons due to the accumulation of oxygen species (O_2^-, O^- and O^{2-}) emanating from air which is responsible for the increase of resistance and the reduction of gas content. The entire surface of the film is covered with adsorbed oxygen ions, which reacts with H_2S gas.

Figure 3(B) displays the sensing characteristics of NiO-MnO_2 thin films, which were annealed at 350, 450 and 550 °C, when exposed to H_2S gas at three specific chamber temperatures: 150, 250, and 350 °C. The graph delineates a trend of increasing sensing capability followed by a peak and subsequent decline. At lower chamber temperatures (150 °C), the sensing characteristic is notably subdued. This can be attributed to the inert nature of H_2S gas molecules at this temperature, impeding their ability to surpass the activation energy barrier required for reaction with adsorbed oxygen molecules. Conversely, at 250 °C, a heightened sensing response is observed. This surge could be attributed to the increased energy available to gas molecules, thereby accelerating the reaction process. However, at higher temperatures such as 350 °C, gas molecules exhibit rapid dispersal from the thin film surface, rendering them ineffectual in altering the sensor's conductivity and resulting in a diminished response.

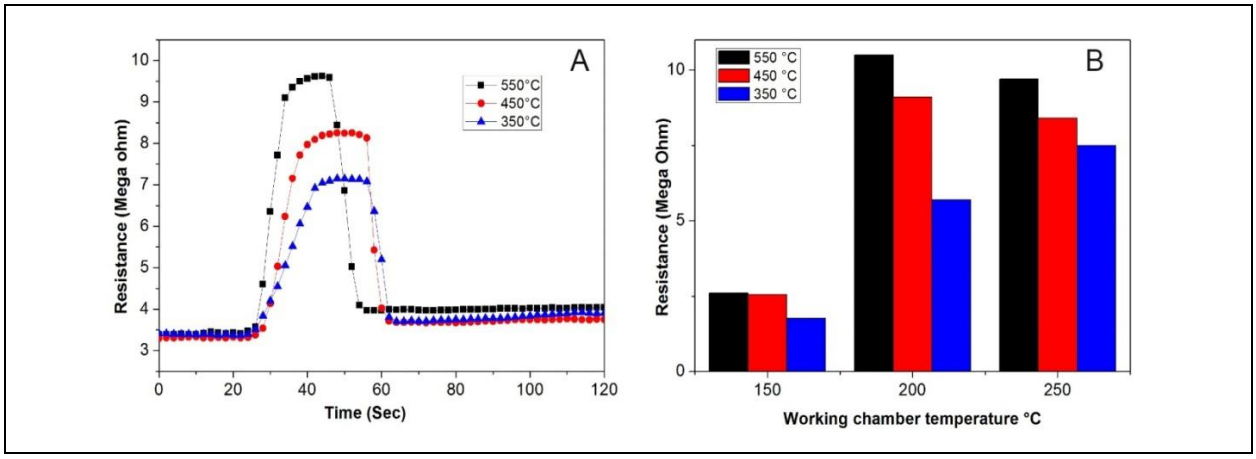

Fig. 3: A) Response of NiO-MnO_2 thin films to 100 ppm H_2S gas at 250 °C B) Sensing characteristics of NiO-MnO_2 thin films annealed at 350, 450, and 550 °C when exposed to H_2S gas at chamber temperatures of 150, 250, and 350 °C

Table 1. Comparing H_2S gas responses of metal oxide sensors

Material	Method of preparation	H_2S Gas concentration	Annealed Temperature	Response	Reference
NiO-MnO_2	Jet nebulizer spray deposition	100 ppm	550 °C	165	This work
CuO-WO_3	Thermal evaporation	100 ppm	300 °C	208	Park *et al*. 2014
Cu-ZnO	Spray pyrolysis	20 ppm	250 °C	38	Shewale *et al*. 2013
$NiMn_2O_4$	Solvent evaporation method	2 ppm	500 °C	-	Guan *et al*. 2014
CuO/NiO/Bi_2O_3–SnO_2	Dip-coating	80 ppm	50 °C	417	Zhou *et al*. 2011

Table 1 compares various sensors against the sensors prepared in this study, which indicates that the NiO-MnO_2 sensor prepared by annealing at 550 °C for 2 hours exhibits a high sensitivity (165), along with shorter response (10 seconds) and recovery time (10 seconds). Sensitivity measures measures how effectively the sensor can detect the presence of the target analyte. High sensitivity implies that even small concentrations of the analyte can be detected. Response Time is the time taken for the sensor to reach a stable signal after the analyte is introduced. Short response times indicate that the sensor can quickly detect and respond to changes in analyte concentration. Recovery Time is the time required for the sensor to return to its baseline or original state after the analyte is removed. Short recovery times suggest that the sensor can quickly return to its initial state and be ready for subsequent measurements.

The high sensitivity (165) of the NiO-MnO2 sensor annealed at 550°C is attributed to the optimal balance of material properties achieved at this temperature, which likely enhances the crystal structure and surface morphology, thus increasing active sites for analyte interaction. The shorter response time (10 seconds) and recovery time (10 seconds) reflect the sensor's efficiency in quickly detecting and disengaging from the analyte. This is due to ideal surface characteristics for rapid adsorption and desorption, favorable electrical properties that enhance charge transfer, and material stability that ensures quick adjustments and recovery without excessive crystallization or grain growth.

It was observed that as the annealing temperature increased, so did the sensing response of the thin film. This fluctuation in sensing response can be attributed to structural and morphological alterations induced by varying annealing temperatures. With higher annealing temperatures, the thin film exhibited enhanced crystallinity and a more porous structure, both conducive to improved sensing capabilities.

4. CONCLUSION

In conclusion, the study successfully demonstrated the synthesis and characterization of NiO-MnO_2 thin films through a jet nebulizer spray pyrolysis technique. The thin films, annealed at varying temperatures, exhibited enhanced surface morphology and structural properties as confirmed by scanning electron microscopy, XRD, and UV spectroscopy. Significantly, these films were utilized as efficient gas sensors for hydrogen sulfide detection. The NiO-MnO_2 sensor achieved a remarkable gas-sensing response of 165 when exposed to 100 ppm of hydrogen sulfide gas, accompanied by an impressive response time of 10 seconds. Mechanistic insights into the gas-sensing behavior were comprehensively discussed, elucidating the factors contributing to the superior performance of the NiO-MnO_2 thin film sensor. From a broader

perspective, the developed NiO-MnO_2 thin film sensors represent a significant advancement in gas-sensing technology, offering a promising platform for the sensitive and rapid identification and monitoring of hydrogen sulfide gas. This research contributes to the growing field of nanomaterial-based sensors and underscores their potential for real-world applications in environmental monitoring and industrial safety.

ACKNOWLEDGEMENT

The UGC (MRP-5394/14 (SERO/UGC) March 2014) provided crucial support to the authors for material synthesis. The authors used facilities for material analysis and characterisation provided by Sri Ramakrishna Mission Vidyalaya College of Arts and Science, Coimbatore, Alagappa University, Karaikudi, India.

FUNDING

There is no funding source.

CONFLICT OF INTEREST

The authors declared no conflict of interest in this manuscript regarding publication.

COPYRIGHT

RERFERENCE

Balamurugan, S., Rajalakshmi, A. and Balamurugan, D., Acetaldehyde Sensing Property of Spray Deposited β-MnO2 Thin Films, *J. Alloys Compd.*, *650*, 863-870 (2015). https://doi.org/10.1016/j.jallcom.2015.08.063

Betty, C. A., Choudhury, S. and Shah, A., Nanostructured Metal Oxide Semiconductors and Composites for Reliable Trace Gas Sensing at Room Temperature, *Surfaces and Interfaces*, *36*, 102560 (2023). https://doi.org/10.1016/j.surfin.2022.102560

Chaudhari, G. N., Bambole, D. R., Bodade, A. B. and Padole, P. R., Characterization of Nanosized TiO_2 Based H_2S Gas Sensor, *J Mater Sci*, *41* (15), 4860–4864 (2006). https://doi.org/10.1007/s10853-006-0042-7

Della Gaspera, E., Bello, V., Mattei, G. and Martucci, A., SiO_2 Mesoporous Thin Films Containing Ag and NiO Nanoparticles Synthesized Combining Sol–Gel and Impregnation Techniques, *Mater. Chem. Phys.*, *131* (1–2), 313–319 (2011). https://doi.org/10.1016/j.matchemphys.2011.09.047

Din, S. U., Haq, M. U., Sajid, M., Khatoon, R., Chen, X., Li, L., Zhang, M. and Zhu, L., Development of High-Performance Sensor Based on NiO/SnO_2 Heterostructures to Study Sensing Properties towards Various Reducing Gases, *Nanotechnol. 31* (39), 395502 (2020). https://doi.org/10.1088/1361-6528/ab98bb

Guan, Y., Yin, C., Cheng, X., Liang, X., Diao, Q., Zhang, H. and Lu, G. Sub-Ppm H_2S Sensor Based on YSZ and Hollow Balls $NiMn_2O_4$ Sensing Electrode. *Sens. Actuators B: Chem. 193*, 501–508. (2014). https://doi.org/10.1016/j.snb.2013.11.072

Guisbiers, G., Mejía-Rosales, S. and Leonard Deepak, F., Nanomaterial Properties: Size and Shape Dependencies, *J. Nanomater.*, *2012*, 1–2 (2012). https://doi.org/10.1155/2012/180976

He, L. and Ling, Z., Studies of Temperature Dependent Ac Impedance of a Negative Temperature Coefficient Mn-Co-Ni-O Thin Film Thermistor, *Appl. Phys. Lett.*, *98* (24), 242112 (2011). https://doi.org/10.1063/1.3596454

Hu, J., Yang, J., Wang, W., Xue, Y., Sun, Y., Li, P., Lian, K., Zhang, W., Chen, L., Shi, J. and Chen, Y., Synthesis and Gas Sensing Properties of NiO/SnO2 Hierarchical Structures toward Ppb-Level Acetone Detection, *Mater. Res. Bull.*, *102*, 294–303 (2018). https://doi.org/10.1016/j.materresbull.2018.02.006

Huang, Z., Zhou, W., Ouyang, C., Wu, J., Zhang, F., Huang, J., Gao, Y. and Chu, J., High Performance of Mn-Co-Ni-O Spinel Nanofilms Sputtered from Acetate Precursors, *Sci. Rep.*, *5* (1), 10899 (2015). https://doi.org/10.1038/srep10899

Jagadeesan, V. and Subramaniam, V., Development of an Automated Nebulizer Spray Pyrolysis System and Its Application in the P-N Junction Diode Fabrication, *J. Phys.: Conf. Ser.*, *1921* (1), 012009 (2021). https://doi.org/10.1088/1742-6596/1921/1/012009

Kumar, R., Kumar, R., Kushwaha, N. and Mittal, J., Ammonia Gas Sensing Using Thin Film of MnO_2 Nanofibers, *IEEE Sensors J.*, *16* (12), 4691–4695 (2016). https://doi.org/10.1109/JSEN.2016.2550079

Paine, D. C., Whitson, T., Janiac, D., Beresford, R., Yang, C. O. and Lewis, B., A Study of Low Temperature Crystallization of Amorphous Thin Film Indium–Tin–Oxide, *J. Appl. Phys.*, *85* (12), 8445–8450 (1999). https://doi.org/10.1063/1.370695

Park, S., Park, S., Jung, J., Hong, T., Lee, S., Kim, H. W. and Lee, C., H_2S Gas Sensing Properties of CuO-Functionalized WO3 Nanowires, *Ceram. Int.*, *40* (7), 11051–11056 (2014). https://doi.org/10.1016/j.ceramint.2014.03.120

Patterson, A. L., The Scherrer Formula for X-Ray Particle Size Determination, *Phys. Rev.*, *56* (10), 978–982 (1939). https://doi.org/10.1103/PhysRev.56.978

Sethupathi, N., Thirunavukkarasu, P., Vidhya, V. S., Thangamuthu, R., Kiruthika, G. V. M., Perumal, K., Bajaj, H. C. and Jayachandran, M., Deposition and Optoelectronic Properties of ITO (In_2O_3:Sn) Thin Films by Jet Nebulizer Spray (JNS) Pyrolysis Technique, *J. Mater. Sci.: Mater. Electron.*, *23* (5), 1087–1093 (2012). https://doi.org/10.1007/s10854-011-0553-0

Shewale, P. S., Patil, V. B., Shin, S. W., Kim, J. H. and Uplane, M. D., H2S Gas Sensing Properties of Nanocrystalline Cu-Doped ZnO Thin Films Prepared by Advanced Spray Pyrolysis, *Sens. Actuators B Chem.*, *186*, 226–234 (2013). https://doi.org/10.1016/j.snb.2013.05.073

Walker, J. M., Akbar, S. A. and Morris, P. A., Synergistic Effects in Gas Sensing Semiconducting Oxide Nano-Heterostructures: A Review, *Sens. Actuators B Chem.*, *286*, 624–640 (2019). https://doi.org/10.1016/j.snb.2019.01.049

Zao, Y., Li-Miao L., Qing W., Quan-Hui L. and Tai-Hong W., High-performance ethanol sensing based on an aligned assembly of ZnO nanorods, Sens Actuators B Chem., 135 (1), 57-60 (2008). https://doi.org/10.1016/j.snb.2008.07.016

Zhou, D., Gan, L., Gong, S., Fu, Q. and Liu, H., P-Type Metal Oxide Doped SnO_2 Thin Films for H_2S Detection, *Sen. Lett.*, *9* (2), 651–654 (2011). https://doi.org/10.1166/sl.2011.1583